# Nature-Based Solutions in Mountain Catchments Reduce Impact of Anthropogenic Climate Change on Hydrological Drought Severity

**Petra Holden** ( petra.holden@uct.ac.za )
University of Cape https://orcid.org/0000-0002-3047-1407

**Alanna Rebelo**
Stellenbosch University

**Piotr Wolski**
University of Cape Town, Cape Town, South Africa https://orcid.org/0000-0002-6120-6593

**Romaric Odoulami**
University of Cape Town https://orcid.org/0000-0001-8228-1608

**Kamoru A. Lawal**
University of Cape Town https://orcid.org/0000-0002-8198-8844

**Joyce Kimutai**
University of Cape Town and Kenya Meteorological Department

**Tiro Nkemelang**
University of Cape Town and Initiative and Botswana Institute for Technology Research and Innovation (BITRI)

**Mark New**
University of Cape Town https://orcid.org/0000-0001-6082-8879

**Article**

**Keywords:** Nature-based Solutions, anthropogenic climate, joint-attribution, hydro-climatic risk

**Posted Date:** September 28th, 2021

**DOI:** https://doi.org/10.21203/rs.3.rs-902740/v1



**Version of Record:** A version of this preprint was published at Communications Earth & Environment on March 9th, 2022. See the published version at https://doi.org/10.1038/s43247-022-00379-9.

# Abstract

Attributing the extent to which Nature-based Solutions (NbS) can offset emerging risk from anthropogenic climate change is a test of effectiveness for climate change adaptation, but has rarely, if ever, been done. Here we show that a widely applied NbS in South Africa – invasive alien tree clearing – can reduce the impact on hydrological drought severity due to human influence on climate, using the Cape Town "Day Zero" drought as an example. Using a multi-model "joint-attribution" framework of coupled climate and landscape states, we find that 12–29% of the hydrological drought severity can be attributed to anthropogenic climate change, compared to 7–15% for reduced rainfall and 1.6-2% for increased reference evapotranspiration. Attributable human influence on meteorological drought was amplified by 5–14% as it propagated through the hydrological system. Clearing invasive alien trees and preventing spread significantly reduced the attributable human influence on hydrological drought severity (2–15% for moderately and 10–27% for fully invaded catchments) but was not sufficient to remove the climate change impact completely. The relative contribution of NbS to drought severity reduction will decrease as climate change progresses. NbS will continue to be important but should be combined with other adaptation options to manage increasing hydro-climatic risk.


# 1. Introduction

The climate is changing due to anthropogenic emissions of greenhouse gasses, and with it extreme weather events, such as droughts and floods[1,2]. Nature-based solutions (NbS), including ecosystem management, protection and restoration, have been proposed for buffering societies from increased risk of climate-related extremes[3–5]. Examples include restoring or protecting riverbanks, wetlands and catchment headwaters to reduce erodibility, ensure water security through increasing water yields, and protect communities from flooding from rainfall extremes[6,7].

Despite the popularity of NbS in policy and research, including the growing literature on the use of NbS as an adaptation response for moderating the impact of human-induced climate change on extremes, there is very little quantitative evidence of their effect on climate risk reduction[8–11]. Nature-based Solutions analyses often focus on climate change mitigation potential with a focus on how much carbon they can remove from the atmosphere[12–14], or more recently NbS effects on global temperatures[15]. These analyses are mostly global despite the scale at which the impacts of anthropogenic climate change on extremes are felt and at which climate adaptation decisions are made. This makes it difficult for results to directly inform regional and local level decision making processes[2].

Quantifying the impact of NbS on the role of anthropogenic climate change on the characteristics of an individual extreme event, such as its intensity, severity, spatial extent, duration, and return interval, is challenging. This is due to a lack of sampling distribution, as we only experience one extreme event i.e., in a world with greenhouse gasses emissions, and no counterfactual i.e., in a world with no human influence on atmospheric conditions. Also, no single event can be attributed to anthropogenic climate change alone. Every extreme weather event is unique and always the result of a combination of both

human-induced and natural drivers as well as internal climate variability. This makes it impossible to say that an event could not have occurred without anthropogenic influence. However, the presence of anthropogenic climate change can alter the characteristics of the extreme weather event[16]. We need methods to be able to quantify the role of anthropogenic climate change in changing extreme event characteristics from a meteorological perspective that can also be used to quantify the role that NbS play in moderating this impact. The science of extreme weather and climate event attribution provides a promising framework to achieve this. Over the last few years, significant advances have been made in this field[2].

There are now numerous examples of probabilistic extreme weather and climate event attribution studies, which have quantified the extent to which human-induced climate change altered the characteristics of a specific extreme event[17,18]. The framework of event attribution has been developed and applied primarily for meteorological events[19]. For example, attribution studies have focused on physical climate variables associated with specific extremes such as rainfall, temperature, or relevant indices that use these variables. A few studies have gone further to determine the extent to which the impact of human influence on the climate modulates impacts on extremes related to hydrological systems or society e.g., flooding in the United Kingdom[20–22] and Okavango[23], streamflow in the USA[24] and human mortality associated with heat waves in Paris and London[25].

We draw on the advances made in the field of attribution science and apply them to attribute the potential for NbS to moderate the impact of anthropogenic climate change on the Cape Town 'Day Zero' drought (2015–2017), a very rare event and the worst in the region since 1904[26,27]. Evidence shows that anthropogenic climate change increased the likelihood of the meteorological drought by a factor of three[28]. Here we focus on a widely implemented NbS in South Africa: Invasive Alien Tree (IAT) clearing. Invasive Alien Trees are a major threat to water security especially in the Western Cape of South Africa. They have spread along rivers and into mountains and have been shown, through paired-catchment and modelling studies, to use significantly more water in comparison to the native shrublands[29]. We assess the relative contribution of anthropogenic climate change and catchment IAT state on hydrological drought severity; and the extent to which management of IATs - through clearing or maintenance and preventing spread - might be able to reduce anthropogenic climate risk.

# 2. Methods

# 2.1 Experimental setup

To quantify the relative fraction of the severity of the hydrological drought attributable to anthropogenic climate change and Invasive Alien Tree (IAT) clearing or lack thereof, we applied a joint probabilistic event attribution framework (Fig. 1) to two shrubland subcatchments - Upper Berg Dam (78 $km^2$) and Du Toits (46 $km^2$) - which supply water impoundments of critical importance to the metropolitan area of Cape Town, the surrounding rural communities and irrigated agriculture in the region (Fig. 2).

We used a multi-model event attribution approach[16,17] but extended this by using linked climate and hydrological model simulations, respectively, of plausible meteorological and hydrological drought conditions in today's climate (referred to as 'Actual') with anthropogenic emissions and a counterfactual climate (referred to as 'Natural') with human-induced drivers removed. We then adjusted the landscape states in the hydrological model to evaluate different combinations of climate and catchment IAT state (referred to as Climate-IAT states). Using this linked climate and hydrological simulation framework, allowed the assessment of: i) how the attributable human influence on the climate and meteorological drought propagate through the terrestrial hydrological system to alter hydrological drought severity; and ii) how subcatchment IAT management (or absence) can modulate the anthropogenic climatically driven drought severity (Fig. 1 and Table 1).

Table 1

**A description of the Climate-Invasive Alien Tree states (Climate-IAT states).** For the climate states, the Actual conditions represented the climate for the drought as we experienced it whereas the Natural conditions represented the drought as it might have been without human influence on atmospheric composition.

| Climate-IAT states | Abbrev. | Description |
|---|---|---|
| Natural + Current | NC | Natural (N) climate state with Current (C) (2019) levels of IATs (9% - Upper Berg; 40% Du Toits) |
| Actual + Current | AC | Actual (A) climate state with Current (C) (2019) levels of IATs (9% Upper Berg; 40% Du Toits) |
| Actual + Invaded | AI | Actual (A) climate state with subcatchments fully Invaded (I) with IATs in areas available for invasion (90% Upper Berg; 98% Du Toits) |
| Actual + Cleared | ACL | Actual (A) climate state with subcatchments fully Cleared (CL) of IATs from the current state |

Climate simulations were derived from 68 ensemble members from the Hadley Centre Regional Model (HadRM3P) nested in the Hadley Centre Global Atmospheric Model (HadAM3P-N96) from the weather@home modelling system (referred to as W@home); 50 ensemble members from one model (ECHAM5.4) from the Climate of the 20th Century Plus (C20C+) Detection and Attribution project (referred to as C20C); and one ensemble member for each of 27 Coupled General Circulation Models from the fifth phase of the Coupled Models Intercomparison Project (referred to as CMIP5) (Sect. 2.4).

For the IAT states, the 'Current' state (C), represented the observed IAT cover during the drought period, which was 9% for the Upper Berg and 40% for the Du Toits, as was derived from Sentinel 2 satellite imagery for January 2019 (described in[30]). The 'Invaded' state (I) represented a scenario in which the subcatchment had become fully invaded, and this had persisted over the drought period; and the 'Cleared' state (CL) represented a scenario where all the IATs in the subcatchments had been cleared prior to the drought years and the subcatchment remained free of IATs (Fig. 3).

Each coupled Climate-IAT state was represented through an ensemble of 145 simulations (alternative realisations) of the climate during the 2015–2017 drought with (Actual) and without (Natural) human influence on atmospheric composition for three different Invasive Alien Tree (IAT) states. For each coupled Climate-IAT state, we simulated daily streamflow in cubic meters per second (cumecs) for the drought period, 2015–2017 (Fig. 1 and Table 1, Supplementary Fig. 1). This resulted in a total of 580 simulations of the hydrological response of the system.

To determine how the severity of the drought changed between respective Climate-IAT states, we calculated a Severity Ratio (SR) (Table 2):

$SR = S_0 / S_i$ (1)

where $S_0$ is the simulated mean daily streamflow during the drought period with Natural climate and Current IAT state (NC), and $S_i$ is the streamflow for different combinations of Actual-IAT states (-Current [AC], Invaded [AI] and Cleared [ACL]).

For the Natural Current (NC) and Actual Current (AC) Climate-IAT combination, SR > 1 indicates that anthropogenic climate change has increased the severity of the hydrological drought. To determine the percentage change in the severity of the drought attributable to anthropogenic climate change, we calculated the Fraction of Attributable Severity (FAS) (Table 2):

$FAS = (1 - 1/SR) * 100$ (2)

For the Natural Current (NC) and Actual Current (AC) Climate-IAT combination, a FAS of 100% indicates that the drought is entirely attributable to anthropogenic climate change while 0% indicates no attributable influence. Negative values indicate that anthropogenic climate change has resulted in the decrease in the severity of the drought. This approach builds on[31] but instead of the term magnitude (which they use for seasonal rainfall maxima) we use the term severity because our focus is on low flows.

Table 2

**Severity Ratio (SR) and Fraction of Attributable Severity (FAS) equations for Climate-IAT states.** This table presents the structure of the equations used to isolate the impact of Anthropogenic Climate Change (ACC) in relation to Invasive Alien Tree (IAT) clearing or lack thereof.

| No. | Climate-IAT state names | Code | SR | FAS | Constant | Impact |
|---|---|---|---|---|---|---|
| 1 | Natural + Current /Actual + Current | NC/AC | $S_0/S_{i-AC}$ | $(1-1/(S_0/S_{i-AC}))$ *100 | Current IAT | ACC only |
| 2 | Natural + Current /Actual + Invaded | NC/AI | $S_0/S_{i-AI}$ | $(1-1/(S_0/S_{i-AI}))$ *100 | none | ACC + Invaded IAT |
| 3 | Natural + Current /Actual + Cleared | NC/ACL | $S_0/S_{i-CLA}$ | $(1-1/(S_0/S_{i-CLA}))$ *100 | none | ACC + Cleared IAT |

The difference between the SR and FAS calculated for the Natural Current in relation to the Actual Current and the other two Climate-IAT states (Actual Invaded and Actual Cleared) shows the extent to which IAT clearing or the lack thereof could moderate or exacerbate the impact of anthropogenic climate change on the severity of the hydrological drought. It also shows the change in the Fraction of Attributable Severity given anthropogenic climate change that can be attributed to IAT clearing or the lack thereof (Table 3).

Table 3

**Calculating the potential to modulate the impact of anthropogenic climate change.** The equations used to determine the extent to which Invasive Alien Tree (IAT) clearing or the lack thereof could have played a role in moderating the impact of Anthropogenic Climate Change (ACC) on the severity of the drought (2 – 1 and 3 – 1 in the column Diff refers to Table 2 above).

| Diff | SR diff | FAS diff | Impact Diff | SR diff description | FAS diff description |
|---|---|---|---|---|---|
| 2 – 1 (NC/AI – NC/AC) | $S_0/S_{i-AI}$ - $S_0/S_{i-AC}$ | $((1-1/(S_0/S_{i-AI}))$ *100)) - $((1-1/(S_0/S_{i-AC}))$ *100)) | (ACC + Invaded IAT) - ACC | Extent to which IATs exacerbated or reduced the impact of ACC | Change in the Fraction of Attributable Severity given ACC that can be attributed to the clearing of IATs or the lack thereof |
| 3 – 1 (NC/ACL – NC/AC) | $S_0/S_{i-ACL}$ - $S_0/S_{i-AC}$ | $((1-1/(S_0/S_{i-ACL}))$ *100)) - $((1-1/(S_0/S_{i-AC}))$ *100)) | (ACC + Cleared IAT) - ACC | | |

To calculate uncertainty for each simulated streamflow for each Climate-IAT state we used a bootstrapping approach to resample the simulations from each climate model experiment resulting in a sample size of 1000 for each Climate-IAT state per climate model experiment (Supplementary Sect. 2). To summarise the results, for each climate model experiment and Climate-IAT state we calculated the

median and 95% quantiles (0.025–0.975 quantiles, referred to as 95% Confidence Intervals [95%CI]). We generated a synthesis of the results across climate model experiments using the mean of the medians for each climate model experiment, with equal weighting, along with 95% confidence intervals generated using the pooled standard deviation of the climate model experiments[32]. We also conducted the same attribution analysis and bootstrapping approach for the rainfall and reference evapotranspiration hydrological model input data. The SR equation for reference evapotranspiration was inverted to $S_i/S_0$ to account for the fact that greater reference evapotranspiration results in higher evaporative demand and more severe drought (Supplementary Sect. 3).

# 2.2 Subcatchments

The Du Toits and Upper Berg are upland shrubland covered subcatchments draining into the Berg and Breede Rivers in the southwestern Cape of South Africa (Table 4). Both subcatchments are extremely mountainous and form part of South Africa's strategic water source areas providing high natural runoff and supporting the region's population and economy. Strategic water source areas only cover 8% of South Africa but contribute substantially to development needs[33]. The Upper Berg and Du Toits provide a critical source of water to the Western Cape Water Supply System, an integrated system of six large water impoundments which supply the City of Cape Town metropolis (58%), the agriculture sector (26%), smaller towns and nearby municipalities (6%), with ~ 10% lost to evaporation[34]. The Upper Berg subcatchment is the main source for the Berg Dam while the Du Toits is one of the main sources for the Theewaterskloof Dam. The Berg and Theewaterskloof Dams account for 15 and 53% of the Western Cape Water Supply System respectively[35]. The lack of rainfall experienced during 2015–2017 in both subcatchments manifested as hydrological drought with streamflow diminishing by 33% (Du Toits) and 54% (Upper Berg) of the long-term average. Both subcatchments were invaded to differing degrees by IATs during the drought period (Fig. 2 and Table 4).

The native vegetation of the region is known as fynbos, which is dominated by sclerophyllous, evergreen shrubs and graminoids, with no tree element except in ravines. Geology is typical of the mountains of the Cape Folded Belt of the Table Mountain Group and soils consist largely of sandstone-quartzitic soils which are highly leached and nutrient poor[36]. The climate is Mediterranean and characterized by winter rainfall. The subcatchments are relatively untransformed and undeveloped except for the IAT invasions which consist mostly of *Acacia mearnsii*, *Pinus spp*, and *Acacia longifolia* (Table 4).

# 2.3 Hydrological model set-up and validation

## 2.3.1 Model set up

The details of the model set up and evaluation are described in[37]. We provide a summary here. We set up MIKE-SHE coupled with MIKE HYDRO River system to simulate the hydrological response of subcatchments to the four coupled Climate-IAT states at a daily time step. MIKE SHE is a physically based modelling system, which can be coupled to MIKE-Hydro River to simulate channel flow. MIKE SHE has five process-oriented components of relevance to our two subcatchments: evapotranspiration (ET),

overland and channel flow, unsaturated and saturated subsurface flows, and exchange between aquifers and rivers.

We used a fully-distributed implementation of MIKE SHE for both subcatchments to represent these major hydrological processes and their interactions. This entailed horizontally and vertically discretizing the subcatchments into an orthogonal network of three-dimensional grid squares (referred to as finite difference cells) to represent the spatial horizontal and vertical variability of subcatchment characteristics and input data. The model cell discretization was 60m with a total of 32 400 and 48 400 cells for the Du Toits and Upper Berg respectively. The vertical depth of the saturated zone on average was 700m and 900m respectively for the Berg and Du Toits but this was distributed spatially based on existing estimated depth information on the Peninsula formation of the Table Mountain Aquifer Group for the region[38–40].

Table 4

**Subcatchment characteristics.** Characteristics of the two subcatchments for which the coupled climate-IAT states were modelled.

| Subcatchment | Upper Berg | Du Toits | Source |
|---|---|---|---|
| Area (square kilometers) | 78 $km^2$ | 46 $km^2$ | Calculated for subcatchments derived from[41] and[42] |
| Altitude (masl) | 761 | 957 | ALOS DSM: Global 30m[42] |
| Mean slope (degrees) | 27 | 23 | |
| Relief roughness (‰): > 160 = extremely dissected | 279 | 246 | [43,44] |
| Mean annual rainfall (mm) | 2553 | 1648 | Estimated from various rainfall gauges and a distributed lapse rate[37] |
| Observed mean daily streamflow at gauges 2004–2017, 2015–2017 (% diff) ($m^3/s$) | 2.2, 1.2 (-45%) | 1.2, 0.8 (-33%) | H6H007 Du Toits for subcatchment<br>G1H076 Berg for one tributary[45] |
| Simulated daily streamflow at gauges 2004–2017, 2015–2017 (% diff) ($m^3/s$) | 2.2, 1.3 (-45%) | 1.0, 0.7 (-30%) | Section 2.3 and [37] |
| Simulated streamflow at subcatchment outlet 2004–2017, 2015–2017 ($m^3/s$) | 4.2, 2.4 (-46%) | See above - gauge is at the outlet | |
| Observed reference evapotranspiration 2004–2017 (station) (mm/day) | 4.1 | | Observed: Penman Monteith reference evapotranspiration (local automatic weather station data ARC 30890) |
| Invasive Alien Tree infestation during drought years (%) | 9 | 40 | Derived at a 20m X 20m resolution from Sentinel 2 imagery[30] |
| Native Fynbos Shrubland high density during drought years (%) | 36 | 23 | |
| Native Fynbos Shrubland low density during drought years (%) | 43 | 35 | |
| Other land cover (bare, indigenous forest, wetland, urban, water, rock) (%) | 7.7 (0.6; 0.5; 0.9; 0; 5.1; 0.6) | 2.9 (0.1; 0.3; 0.1; 0.2; 0; 2.2) | |

The overland flow zone was characterised based on land use and land cover data derived from Sentinel 2 imagery[30]. Three main computational layers were used with variable thicknesses to describe vertical

variations in the subsurface and their respective hydrogeological characteristics within each grid square. This included the unsaturated soil zone (1.5 m deep), the saturated zone (15m deep), including a perched talus and weathered sandstone aquifer to mimic subsurface piston flow typical of these subcatchments[46], and a spatially distributed deep Peninsula Aquifer.

Characteristics and parameterisations for the overland flow zone and subsurface layers were derived from various approaches including field sampling and laboratory analyses (unsaturated zone soil properties including soil depths, parameter values for the van Genuchten model, river channel cross sections, and Leaf Area Indices) and literature review combined with calibration processes (saturated zone layers, depths, horizontal and vertical hydraulic properties, specific storage and yields). Algorithms used included the Kristensen and Jensen equations to calculate actual transpiration and soil evaporation based on several evapotranspiration parameters; diffusive wave approximation of the Saint Venant equations based on the finite difference formulation for overland flow, vertical flow in the soil zone was modeled using Richards' Equation, which solves for pressure head variation in the unsaturated zone; and groundwater flow in the saturated zone was modelled using the three dimensional Darcy equation.

We linked the overland flow and groundwater flow modules in MIKE SHE to a channel network by coupling with the MIKE Hydro River hydrodynamic river module. This coupling enabled one-dimensional simulation of river flows and water levels using the fully dynamic Saint Venant equations.

### 2.3.2 Hydrological model validation

Both Upper Berg and Du Toits subcatchment models performed satisfactorily[47], with less than 9% difference in daily mean flow compared to observations and including Nash-Sutcliffe efficiencies of above 0.58 (logged: 0.74), r values greater than 0.77 and PBIAS between − 4 and − 10 for daily data (Supplementary Fig. 7, Table 4; for the full description of the model set up and parameterisations see[37]).

## 2.4 Climate change attribution hydrological inputs

### 2.4.1 Climate models and states

We used 29 General Circulation Models (GCMs); 27 Coupled and 2 Atmospheric, and from these 290 simulations of the south-western Cape drought (1 January 2015 to 31 December 2017). Simulations represented two climate states: i) Actual (145 simulations); and ii) Natural (145 simulations) (Table 5).

Atmospheric General Circulation Models (AGCMs) are prescribed with Sea Surface Temperatures (SSTs) to isolate the component of atmospheric variability driven by oceanic boundary forcing by eliminating the influence of the atmosphere on the ocean. They are useful for determining how the atmospheric circulation and land-surface climate might respond to a given set of surface boundary conditions[48,49]. On the other hand, Coupled General Circulation Models (CGCMs) allow a dynamically interacting ocean, although simulated SSTs do not necessarily track those observed[50].

Both the C20C and Climate Prediction.net experiments involve running many simulations of AGCMs differing only in their initial conditions and so representing possible trajectories of the climate system under a given set of time-evolving boundary conditions. We used simulations from ECHAM5.4 from the C20C experiment[51,52] as it was the only AGCM in C20C that fully covered the drought period. The Weather@home model from the Climate Prediction.net experiment is a 50km Hadley Centre Regional Model (HadRM3P) for the southern African regional domain nested in the Hadley Centre Global Atmospheric Model (HadAM3P-N96)[53,54].

Table 5

**Climate model data underpinning to two climate states.** Model experiments and number of models and ensemble members used in this study to represent the drought period (2015–2017).

| Model experiments | Model name/s | Models | Climate states (Actual & Natural) | Ensemble members per scenario | Total drought simulations |
|---|---|---|---|---|---|
| **Atmospheric General Circulation Models (AGCMs)** | | | | | |
| Climate Prediction.net distributed computing platform (referred to as W@home) | Weather@home | 1 | 2 | 68 | 136 |
| Climate of the 20th Century Plus (C20C+) Detection and Attribution project (referred to as C20C) | ECHAM5.4 | 1 | 2 | 50 | 100 |
| **Coupled General Circulation Models (CGCMs)** | | | | | |
| Fifth phase of Coupled Model Intercomparison Project (referred to as CMIP5) | Supplementary Table 5 | 27 | 2 | 27 | 54 |
| Totals | | 29 | | 145 | 290 |

For the AGCMs, Actual simulations represented plausible realisations of the drought (in this case precipitation and daily temperature data) under 2015–2017 observed boundary conditions. This included simulations forced by observed sea surface temperature (SST), sea ice concentration (SIC), greenhouse gases (GHG) and aerosols. In contrast, Natural simulations represented possible realisations of the drought in the absence of anthropogenic interference with the climate system. This included naturalised (detrended and adjusted) sea surface temperatures and sea ice concentrations without an anthropogenic climate change signal and pre-industrial greenhouse gases and aerosols (e.g., boundary conditions representing the 1880s) (see https://portal.nersc.gov/c20c/data.html; https://www.climateprediction.net/).

For the CMIP5 CGCMs, we used a combination of the historical runs and future runs from the first ensemble member (r1i1p1) of each of 27 models from the Coupled Model Intercomparison Project 5

(CMIP5) under a high emission scenario (representative concentration pathway 8.5, RCP8.5)[55,56]. To minimise the effect of unforced interannual variability, we extracted 2 periods of 31 years each, 1869–1899 and 2001–2031, representing the Natural and the Actual climate states respectively. For each of these 31 year periods, we then extracted the driest three years based on a three-year running average to represent the drought periods across the models.

## 2.4.2 Climate model evaluation for the hydrological modelling domain

All climate models were evaluated specifically for the southwestern Cape modelling domain using precipitation observations from the University of East Anglia Climate Research Unit (CRU) and reanalysis data from the European Centre for Medium-Range Weather Forecasts (ECMWF – ERA version 5: ERA5). We found that the models were able to reproduce seasonal and spatial variations of the observed rainfall to a satisfactory level, and that bias correction (see below) addressed any major deficiencies affecting the inputs to the hydrological model (Supplementary Fig. 8, 9).

## 2.4.3 Bias correction

We extracted daily precipitation and daily minimum and maximum temperature from each climate model simulation from the corresponding nearest grid point to each rainfall or reference evapotranspiration observed station used to drive the hydrological model. Data were extracted for a period of 15 years (2004–2018) for the AGCMs and 31 years (1869–1899 and 2001–2031) for the CGCMs for both the Actual and Natural climate states. We derived reference evapotranspiration from the temperature data following[57].

Before isolating the drought years (see 2.4.1) for analysis from the climate data and running these in the hydrological models, we bias corrected the climate model data using a standard quantile-quantile bias correction approach[58,59] based on the nearest observed station driving the baseline hydrological model and a 20-day moving window. For the Actual climate state, quantile-quantile bias correction was performed by using a 20-day moving window around each day in all years to generate empirical cumulative distribution functions (ECDF) for the data for both observed station and climate model data. The quantiles for the observed station data were then mapped onto the corresponding model quantiles and the value for the observed data extracted as the new bias corrected daily value. For the Natural climate state, we aligned the daily quantiles for each of the simulations with the corresponding daily quantiles in the climate model data from the Actual climate state, and then used the corresponding observed station quantile value as the bias corrected value. Bias correction further improved the correlations with inter-annual and seasonal variations of local rainfall observation stations (Supplementary Fig. 10, 11).

# 3. Results

We first assess the increase in severity of the hydrological drought attributable to human influence on the climate, under observed (i.e., “current”) Invasive Alien Tree (IAT) state (i.e., NC/AC). The multi-model synthesis mean Severity Ratio (SR) is 1.21 (95%CI: 1.13–1.28) and 1.29 (95%CI: 1.17–1.4) for the Berg and Du Toits, respectively. Simulated results showed that 16.9% (95%CI: 11.6–21.1%) and 22.1% (95%CI: 15.3–29%) of the severity of the hydrological drought during 2015–2017 in these subcatchments can be attributed to anthropogenic climate change in the Berg and Du Toits, respectively. All individual model experiments (C20C, CMIP5, and W@home) also on their own show an attributable increase in severity of the hydrological drought. Synthesis and individual model experiment results are statistically significant as the SR 95% confidence intervals are greater than one in all cases (Fig. 4 and Table 9).

The Fraction of Attributable Severity (FAS) for streamflow was ~ 5–14% and ~ 11–27% larger than that for rainfall and reference evapotranspiration, respectively, over the subcatchments (Supplementary Fig. 2–5 and Table 1–2). This shows that subcatchment hydrological processes exacerbated the anthropogenic climate change signal as it moved from meteorological drought to hydrological drought. Both subcatchments showed a significant impact of anthropogenic climate change on the lack of rainfall, with the multi-model synthesis mean FAS being 10.8% (95%CI: 7.1–14.5) and 10.9% (95%CI: 6.9–14.9) for the Berg and Du Toits respectively (Supplementary Fig. 2–3 and Table 1).

Table 9

**Table format of results shown in** Fig. 4. Median Severity Ratio (SR) and Fraction of Attributable Severity (FAS) (with 95% confidence intervals) for the Upper Berg and Du Toits, shown separately for all model experiments and synthesis across model experiments. NC = Natural Current; ACL = Actual Cleared; AI = Actual Invaded.

| Climate-IAT states | Model | Upper Berg | | Du Toits | |
|---|---|---|---|---|---|
| | | **SR (95% CI)** | **FAS (95% CI)** | **SR (95% CI)** | **FAS (95% CI)** |
| NC/AC | C20C | 1.19 (1.11, 1.28) | 15.7 (9.8, 21.6) | 1.21 (1.1, 1.33) | 17.7 (9.2, 24.8) |
| | CMIP5 | 1.26 (1.17, 1.35) | 20.5 (14.5, 25.7) | 1.37 (1.24, 1.52) | 27.1 (19.6, 34) |
| | W@home | 1.12 (1.07, 1.18) | 10.8 (6.1, 15.2) | 1.2 (1.12, 1.28) | 16.5 (10.4, 21.8) |
| | Synthesis | 1.21 (1.13, 1.28) | 16.9 (11.6, 22.1) | 1.29 (1.17, 1.4) | 22.1 (15.3, 29) |
| NC/ACL | C20C | 1.17 (1.09, 1.26) | 14.6 (8.4, 20.5) | 1.11 (1, 1.21) | 9.6 (0, 17.5) |
| | CMIP5 | 1.24 (1.15, 1.33) | 19.2 (13.3, 25) | 1.22 (1.11, 1.34) | 17.7 (9.6, 25.4) |
| | W@home | 1.11 (1.05, 1.16) | 9.6 (4.7, 13.8) | 1.09 (1.01, 1.16) | 7.9 (1.2, 13.6) |
| | Synthesis | 1.19 (1.11, 1.26) | 15.6 (10.4, 20.9) | 1.16 (1.06, 1.26) | 13.2 (5.9, 20.6) |
| NC/AI | C20C | 1.39 (1.29, 1.5) | 28.2 (22.7, 33.3) | 1.58 (1.41, 1.75) | 36.9 (29.2, 42.9) |
| | CMIP5 | 1.55 (1.44, 1.67) | 35.6 (30.7, 40.3) | 1.98 (1.77, 2.22) | 49.4 (43.6, 55) |
| | W@home | 1.33 (1.26, 1.4) | 24.6 (20.6, 28.6) | 1.56 (1.45, 1.67) | 36 (31.2, 40.2) |
| | Synthesis | 1.46 (1.36, 1.55) | 31 (26.5, 35.6) | 1.77 (1.6, 1.95) | 42.9 (37.5, 48.3) |

We show a small but attributable anthropogenic climate change impact on the increase in reference evapotranspiration with a multi-model synthesis mean FAS of 1.95% (95%CI: 1.68–2.22) (Supplementary Fig. 4–5 and Table 2). Although we do not analyse actual evapotranspiration, it is likely that the attributable influence on actual evapotranspiration would be lower, as reduced rainfall in the drought would limit water available for evaporatranspiration[60]. Furthermore, when we run the hydrological model with and without human influence on reference evapotranspiration, we see that reference evapotranspiration only makes a small difference to the SR and FAS results (Supplementary material Fig. 6 and Table 3). For example, human influence on the climate on the lack of rainfall contributed between 97–99% to the multi-model synthesis mean SR and 85–90% to the multi-model synthesis mean FAS

obtained for NC/AC (Supplementary material Fig. 6 and Table 3). These findings align with previous work which shows it was primarily the lack of rainfall driving the 2015–2017 meteorological drought experienced in the region[28].

We now assess the relative contribution of anthropogenic climate change and IAT extent on the severity of the hydrological drought (Table 3 in 2.1 i.e., NC/AI - NC.AC and NC/ACL - NC/AC). In all cases clearing IATs could not remove the full anthropogenic climate change signal as it propagated through the hydrological system. For example, even with full clearing of both subcatchments there remained a statistically significant effect of anthropogenic climate change on the severity of the hydrological drought (Fig. 4 and Table 9). However, simulations showed that clearing IATs could significantly reduce this impact, depending on the extent of invasion (Fig. 5 and Table 10).

For example, simulations showed that clearing the 40% invaded area in the Du Toits subcatchment before the drought hit in 2015 would have significantly reduced the impact of anthropogenic climate change on the hydrological drought by reducing the FAS by 8.9% (95%CI: -15.4, -2.4). In contrast, clearing the much smaller extent of aliens that were present in the Upper Berg subcatchment would have only reduced the impact of anthropogenic climate change on the severity of the drought by 1.3% (FAS) and this is not significant (95% CI: -5.9, 3.3%). Extensive clearing had already been implemented in the Upper Berg prior to the drought to reduce the invasions down to the current 9% levels in the landscape. This mostly took place between 2006–2010 when the former plantation forestry areas were cleared, but maintenance and follow up clearing have continued from 2010 under South Africa's Working for Water programme[61]. It is therefore likely that if this clearing had not been implemented and maintained, the impacts of anthropogenic climate change on the water shortages in the Berg water impoundment would have been further exacerbated. Furthermore, if invasion had not been managed, and the subcatchments had become fully invaded at the time of drought, the impact of anthropogenic climate change on the drought would have significantly exacerbated the SR by 0.25 (95%CI: 0.17, 0.33) or 0.48 (95%CI: 0.33, 0.64) equating to a FAS of 14.1 (95%CI: 9.6, 18.7) and 20.7% (95%CI: 14.4, 27) and thus increase in the human influence on the severity of the hydrological drought, respectively for the Upper Berg and Du Toits.

Table 10

**Table format of** Fig. 5 **above.** Change in the Severity Ratio (SR) and Fraction of Attributable Severity (FAS) (with 95% confidence intervals) for the Upper Berg and Du Toits due to Invasive Alien Tree management (NC/ACL - NC/AC) or the lack thereof (NC/AI-NC/AC) (see Table 3 in Sect. 2.1). NC = Natural Current; ACL = Actual Cleared; AI = Actual Invaded.

| Diffs | model | Upper Berg (95% PB/*CI*) | | Du Toits (95% PB/*CI*) | |
|---|---|---|---|---|---|
| | | **Change in SR** | **Change in FAS** | **Change in SR** | **Change in FAS** |
| Change if cleared current | C20C | -0.02 (-0.09, 0.06) | -1.2 (-6.2, 4.5) | -0.11 (-0.21, -0.02) | -8.2 (-15.4, -1.1) |
| invasion | CMIP5 | -0.02 (-0.1, 0.07) | -1.4 (-6.6, 4.2) | -0.15 (-0.28, -0.04) | -9.4 (-16.5, -2.4) |
| | W@home | -0.02 (-0.06, 0.03) | -1.3 (-4.8, 2.6) | -0.11 (-0.18, -0.05) | -8.6 (-13.7, -3.6) |
| | Synthesis | -0.02 (-0.09, 0.05) | -1.3 (-5.9, 3.3) | -0.13 (-0.23, -0.03) | -8.9 (-15.4, -2.4) |
| Change if allowed full invasion | C20C | 0.21 (0.12, 0.3) | 12.5 (7.2, 17.9) | 0.37 (0.22, 0.52) | 19 (11.9, 26.6) |
| | CMIP5 | 0.29 (0.2, 0.39) | 15.1 (10.2, 19.9) | 0.6 (0.41, 0.83) | 22.1 (15.5, 29.3) |
| | W@home | 0.21 (0.15, 0.27) | 13.9 (10.1, 17.8) | 0.36 (0.28, 0.46) | 19.6 (14.6, 24.4) |
| | Synthesis | 0.25 (0.17, 0.33) | 14.1 (9.6, 18.7) | 0.48 (0.33, 0.64) | 20.7 (14.4, 27) |

# 4. Conclusion

We fill a gap in the current climate change adaptation literature by providing quantitative and statistically robust evidence that Nature-based Solutions (NbS) can be an important adaptation approach that can support hydro-climate risk reduction. We focus at a scale at which the impacts of climate change on extremes are felt and at which climate adaptation decisions are made[2]. We show the importance of managing vegetation cover in headwater catchments in the Mediterranean climate of the southwestern Cape for reducing the hydrological impact of anthropogenic climate change via extreme meteorological drought events. Despite our regional focus, the results are of relevance to areas across the globe that are experiencing woody encroachment due to IATs or woody indigenous vegetation such as grassland and savanna systems[62–64]. Our results also support existing cautionary warnings for those promoting extensive tree planting in ecoregions that are not comprised of extensive forested landscapes (shrubland, savanna and grassland systems)[4]. This is especially pertinent as current climate models are likely overestimating the removal of atmospheric carbon by forests when compared to other grassy systems[65].

In the context of this study, we show that high cover of IATs (such as the 40% currently occurring in one of our subcatchments or under hypothetical full invasion in both catchments) can significantly exacerbate the impact of anthropogenic climate change on the severity of hydrological drought and resulting water shortages, such as those experienced during the Cape Town Day Zero drought. Furthermore, clearing IATs and maintaining IATs at low levels of invasion can significantly reduce the attributable anthropogenic climate change risk as it propagates through the hydrological system. Thus, continuous maintenance and upscaling of clearing efforts in areas of high invasion is a viable mechanism to adapt to changing hydro-climatic extremes. Efforts directed at strategically important headwater catchments will likely yield high dividends. Within these catchments, our results suggest greater benefit from clearing heavily invaded catchments (such as the 40% occurring in the Du Toits, and greater) and maintenance at low invasion levels (such as maintaining the 9% occurring in the Upper Berg), compared to eradication of IATs in catchments with lower invasion levels (such as completely clearing the 9% occurring in the Upper Berg).

Although two factors drive hydrological drought, rainfall and reference evapotranspiration, no extreme event attribution studies have propagated both as influenced by anthropogenic climate change through a hydrological modelling system to determine attributable hydrological drought severity to anthropogenic climate change. We found a strong attributable influence of climate change on rainfall and a weak but significant influence on reference evapotranspiration. Our results agree with previous work in the region confirming that human influence on reduced rainfall was the dominant driver of the 2015–2017 meteorological drought[28], but we extend this to show it was also the dominant driver of the hydrological drought experienced in these subcatchments.

Nature-based Solutions are important for reducing drought impact but does not completely offset the anthropogenic component of the drought we studied - even at current warming levels and rainfall changes. As we expect meteorological drought risk to increase going forward due to human influence on the climate[28,66], the contribution of NbS to offsetting human influence on drought, while still important, will likely decrease. This finding supports the necessity of understanding the ‘hard limits’[67] of climate change adaptation actions to changing climate conditions and supports the urgency that is required for climate policies to live up to stringent emission reductions. Further research is needed to understand when and under what conditions human influence on the climate will eventually exceed the potential of NbS for reducing hydrological drought risk, while considering different NbS types and contexts across the globe[67,68]. Furthermore, NbS must be fully integrated into a wider portfolio of water security adaptation options.

## Declarations

# Acknowledgements

We are grateful for funding for this research from the AXA Research Fund, through the AXA Research Chair in African Climate Risk, the Danish Ministry of Foreign Affairs (MFA) [grant number 17-M07-KU],

and the BNP Paribas Foundation Climate Initiative. We acknowledge the Agricultural Research Council, South African Weather Service, South African Environment Observation Network, Umvoto and City of Cape Town, and Zutari for data.

# References

1. IPCC. in *Climate Change 2021: The Physical Science Basis. Contribution of Working Group I to the Sixth Assessment Report of the Intergovernmental Panel on Climate Change* (eds V. Masson-Delmotte, P. Zhai, A. Pirani, S. L. Connors, C. Péan, S. Berger, N. Caud, Y. Chen, L. & M. I. Gomis Goldfarb, M. Huang, K. Leitzell, E. Lonnoy, J.B.R. Matthews, T. K. Maycock, T. Waterfield, O. Yelekçi, R. Yu, B. Zhou) (Cambridge University Press. In Press, 2021).
2. Otto, F. E. L. *et al.* Toward an Inventory of the Impacts of Human-Induced Climate Change. *Bulletin of the American Meteorological Society* **101**, E1972-E1979, doi:10.1175/bams-d-20-0027.1 (2020).
3. Cohen-Shacham, E. *et al.* Core principles for successfully implementing and upscaling Nature-based Solutions. *Environmental Science & Policy* **98**, 20-29, doi:10.1016/j.envsci.2019.04.014 (2019).
4. Seddon, N. *et al.* Getting the message right on nature-based solutions to climate change. *Glob Chang Biol*, doi:10.1111/gcb.15513 (2021).
5. Keesstra, S. *et al.* The superior effect of nature based solutions in land management for enhancing ecosystem services. *Sci Total Environ* **610-611**, 997-1009, doi:10.1016/j.scitotenv.2017.08.077 (2018).
6. Seddon, N. *et al.* Understanding the value and limits of nature-based solutions to climate change and other global challenges. *Philos Trans R Soc Lond B Biol Sci* **375**, 20190120, doi:10.1098/rstb.2019.0120 (2020).
7. Gómez Martín, E., Máñez Costa, M. & Schwerdtner Máñez, K. An operationalized classification of Nature Based Solutions for water-related hazards: From theory to practice. *Ecological Economics* **167**, doi:10.1016/j.ecolecon.2019.106460 (2020).
8. Doswald, N. *et al.* Effectiveness of ecosystem-based approaches for adaptation: review of the evidence-base. *Climate and Development* **6**, 185-201, doi:10.1080/17565529.2013.867247 (2014).
9. Chausson, A. *et al.* Mapping the effectiveness of nature-based solutions for climate change adaptation. *Glob Chang Biol*, doi:10.1111/gcb.15310 (2020).
10. Berrang-Ford, L. *et al.* A systematic global stocktake of evidence on human adaptation to climate change. *Research Sqaure* **preprint** (2021).
11. Rebelo, A. J., Holden, P. B., Esler, K. & New, M. G. Benefits of water-related ecological infrastructure investments to support sustainable land-use: a review of evidence from critically water-stressed catchments in South Africa. *R Soc Open Sci* **8**, 201402, doi:10.1098/rsos.201402 (2021).
12. Griscom, B. W. *et al.* Natural climate solutions. *Proc Natl Acad Sci U S A* **114**, 11645-11650, doi:10.1073/pnas.1710465114 (2017).
13. Bastin, J.-F. *et al.* The global tree restoration potential. *Science* **365**, 76-79 (2019).

14. Koch, A., Brierley, C. & Lewis, S. L. Effects of Earth system feedbacks on the potential mitigation of large-scale tropical forest restoration. *Biogeosciences* **18**, 2627-2647, doi:10.5194/bg-18-2627-2021 (2021).
15. Girardin, C. A. J. *et al.* Nature-based solutions can help cool the planet - if we act now. *Nature* **593**, 191-194, doi:10.1038/d41586-021-01241-2 (2021).
16. Otto, F. E. L. Attribution of Weather and Climate Events. *Annual Review of Environment and Resources* **42**, 627-646, doi:10.1146/annurev-environ-102016-060847 (2017).
17. Philip, S. *et al.* A protocol for probabilistic extreme event attribution analyses. *Advances in Statistical Climatology, Meteorology and Oceanography* **6**, 177-203, doi:10.5194/ascmo-6-177-2020 (2020).
18. Herring, S. C., N. Christidis, A. Hoell, M. P. Hoerling, and P. A. Stott. *Explaining Extreme Events of 2019 from a Climate Perspective*. (Bull. Amer. Meteor. Soc., 102 (1), S1–S112, https:/doi.org/10.1175/BAMSExplainingExtremeEvents2019.1, 2021).
19. Otto, F. E. L. *et al.* Challenges to understanding extreme weather changes in lower income countries. *Bulletin of the American Meteorological Society*, doi:10.1175/bams-d-19-0317.1 (2020).
20. Pall, P. *et al.* Anthropogenic greenhouse gas contribution to flood risk in England and Wales in autumn 2000. *Nature* **470**, 382-385, doi:10.1038/nature09762 (2011).
21. Kay, A. L., Crooks, S. M., Pall, P. & Stone, D. A. Attribution of Autumn/Winter 2000 flood risk in England to anthropogenic climate change: A catchment-based study. *Journal of Hydrology* **406**, 97-112, doi:10.1016/j.jhydrol.2011.06.006 (2011).
22. Schaller, N. *et al.* Human influence on climate in the 2014 southern England winter floods and their impacts. *Nature Climate Change* **6**, 627-634, doi:10.1038/nclimate2927 (2016).
23. Wolski, P., Stone, D., Tadross, M., Wehner, M. & Hewitson, B. Attribution of floods in the Okavango basin, Southern Africa. *Journal of Hydrology* **511**, 350-358, doi:10.1016/j.jhydrol.2014.01.055 (2014).
24. Ross, A. C. *et al.* Anthropogenic Influences on Extreme Annual Streamflow into Chesapeake Bay from the Susquehanna River. *Bulletin of the American Meteorological Society* **102** (2021).
25. Mitchell, D. *et al.* Attributing human mortality during extreme heat waves to anthropogenic climate change. *Environmental Research Letters* **11**, 074006, doi:10.1088/1748-9326/11/7/074006 (2016).
26. Botai, C., Botai, J., de Wit, J., Ncongwane, K. & Adeola, A. Drought Characteristics over the Western Cape Province, South Africa. *Water* **9**, doi:10.3390/w9110876 (2017).
27. Wolski, P. How severe is Cape Town's “Day Zero” drought? *Significance* **15**, 24-27 (2018).
28. Otto, F. E. L. *et al.* Anthropogenic influence on the drivers of the Western Cape drought 2015–2017. *Environmental Research Letters* **13**, doi:10.1088/1748-9326/aae9f9 (2018).
29. Van Wilgen, B. W., Measey, J., Richardson, D. M., Wilson, J. R. & Zengeya, T. A. *Biological Invasions in South Africa*. (Springer Nature, 2020).
30. Holden, P. B., Rebelo, A. J. & New, M. G. Mapping invasive alien trees in water towers: A combined approach using satellite data fusion, drone technology and expert engagement. *Remote Sensing*

*Applications: Society and Environment* **21**, doi:10.1016/j.rsase.2020.100448 (2021).

31. Kimutai, J., New, M., Wolski, P. & Otto, F. Attribution of the Human Influence on Heavy Rainfall Associated with Flooding Events during the 2012, 2016, and 2018 March-April-May Season in Kenya. *Journal of Weather and Climate Extremes* (submitted).
32. Paciorek, C. J., Stone, D. A. & Wehner, M. F. Quantifying statistical uncertainty in the attribution of human influence on severe weather. *Weather and Climate Extremes* **20**, 69-80, doi:10.1016/j.wace.2018.01.002 (2018).
33. Nel, J. L. *et al.* Strategic water source areas for urban water security: Making the connection between protecting ecosystems and benefiting from their services. *Ecosystem Services* **28**, 251-259, doi:10.1016/j.ecoser.2017.07.013 (2017).
34. Wolski, P. What Cape Town learned from its drought. *Bulletin of the Atomic Scientists. https://thebulletin.org/2018/04/what-cape-town-learned-from-its-drought/* (2018).
35. DWS. Cape Town River Systems State of Dams on 2021-08-16. *Department of Water and Sanitation. Republic of South Africa. https://www.dws.gov.za/Hydrology/Weekly/RiverSystems.aspx?river=CT* (2021).
36. Manning, J. & Goldblatt, P. *Plants of the greater Cape Floristic Region 1: the Core Cape Flora.*, (South African National Biodiversity Institute, 2012).
37. Rebelo, A. J., Holden, P.B., Hallowes, J., Eady, B., Cullis, J.D., Esler, K.J., New M.G. The hydrological benefits of investing in ecological infrastructure: Alien clearing in the Berg and Breede Catchments, South Africa. *Journal of Hydrology* (submitted).
38. DWAF. *The Assessment of Water Availability in the Berg Catchment (WMA 19) by Means of Water Resource Related Models: Report 9 (Groundwater Model): Volume 9 (Breede River Alluvium Aquifer Model)*. (Department of Water Affairs and Forestry, 2008).
39. DWAF. *The Assessment of Water Availability in the Berg Catchment (WMA 19) by Means of Water Resource Related Models: Report 9 (Groundwater Model): Volume 3 (Regional Conceptual Model)*. (Department of Water Affairs and Forestry, 2008).
40. Blake, D., Mlisa, A. & Hartnady, C. Large scale quantification of aquifer storage and volumes from the Peninsula and Skurweberg Formations in the southwestern Cape. *Water SA* **36**, 177-184 (2010).
41. Tadono, T. *et al.* Generation of the 30 M-Mesh Global Digital Surface Model by Alos Prism. *ISPRS - International Archives of the Photogrammetry, Remote Sensing and Spatial Information Sciences* **XLI-B4**, 157-162, doi:10.5194/isprsarchives-XLI-B4-157-2016 / https://developers.google.com/earth-engine/datasets/catalog/JAXA_ALOS_AW3D30_V3_2#description (2016).
42. Takaku, J., Tadono, T., Tsutsui, K. & Ichikawa, M. Validation of "Aw3d" Global Dsm Generated from Alos Prism. *ISPRS Annals of Photogrammetry, Remote Sensing and Spatial Information Sciences* **III-4**, 25-31, doi:10.5194/isprsannals-III-4-25-2016 (2016).
43. Viviroli, D. Increasing dependence of lowland population on mountain water resources. *Nature Sustainability* **3**, 917–928 (2020).

44. Meybeck, M. A New Typology for Mountains and Other Relief Classes An Application to Global Continental Water Resources and Population Distribution. *Mountain Research and Development* **21** (2001).
45. DWS. Surface water home. *Department of Water and Sanitation. Republic of South Africa. https://www.dws.gov.za/Hydrology/Unverified/UnverifiedDataFlowInfo.aspx* (2021).
46. Midgley, J. & Scott, D. in *Proc. Sixth South African Hydrological Symposium.* 27-34.
47. Moriasi, D. N., Gitau, M.W., Pai, N., Daggupati, P. . Hydrologic and Water Quality Models: Performance Measures and Evaluation Criteria. *Transactions of the ASABE* **58**, 1763-1785, doi:10.13031/trans.58.10715 (2015).
48. Stone, D. A. *et al.* A basis set for exploration of sensitivity to prescribed ocean conditions for estimating human contributions to extreme weather in CAM5.1-1degree. *Weather and Climate Extremes* **19**, 10-19, doi:10.1016/j.wace.2017.12.003 (2018).
49. Risser, M. D., Stone, D. A., Paciorek, C. J., Wehner, M. F. & Angélil, O. Quantifying the effect of interannual ocean variability on the attribution of extreme climate events to human influence. *Climate Dynamics* **49**, 3051-3073, doi:10.1007/s00382-016-3492-x (2017).
50. Jones, G. S., Stott, P. A. & Christidis, N. Attribution of observed historical near-surface temperature variations to anthropogenic and natural causes using CMIP5 simulations. *Journal of Geophysical Research: Atmospheres* **118**, 4001-4024, doi:10.1002/jgrd.50239 (2013).
51. Roesch, A. & Roeckner, E. Assessment of snow cover and surface albedo in the ECHAM5 general circulation model. *Journal of Climate* **19**, 3828-3843 (2006).
52. Roeckner, E. *et al.* Sensitivity of simulated climate to horizontal and vertical resolution in the ECHAM5 atmosphere model. *Journal of Climate* **19**, 3771-3791 (2006).
53. Guillod, B. P. *et al.* weather@home 2: validation of an improved global–regional climate modelling system. *Geoscientific Model Development* **10**, 1849-1872, doi:10.5194/gmd-10-1849-2017 (2017).
54. Massey, N. *et al.* weather@home—development and validation of a very large ensemble modelling system for probabilistic event attribution. *Quarterly Journal of the Royal Meteorological Society* **141**, 1528-1545, doi:10.1002/qj.2455 (2014).
55. Taylor, K. E., Stouffer, R. J. & Meehl, G. A. An Overview of CMIP5 and the Experiment Design. *Bulletin of the American Meteorological Society* **93**, 485-498, doi:10.1175/bams-d-11-00094.1 (2012).
56. Flato, G. *et al.* in *Climate change 2013: the physical science basis. Contribution of Working Group I to the Fifth Assessment Report of the Intergovernmental Panel on Climate Change* 741-866 (Cambridge University Press, 2014).
57. Hargreaves, G. H. & Samani, Z. A. Reference crop evapotranspiration from temperature. *Applied engineering in agriculture* **1**, 96-99 (1985).
58. Cayan, D. R., Maurer, E. P., Dettinger, M. D., Tyree, M. & Hayhoe, K. Climate change scenarios for the California region. *Climatic Change* **87**, 21-42, doi:10.1007/s10584-007-9377-6 (2008).

59. Cannon, A. J., Sobie, S. R. & Murdock, T. Q. Bias correction of GCM precipitation by quantile mapping: How well do methods preserve changes in quantiles and extremes? *Journal of Climate* **28**, 6938-6959 (2015).
60. Dirmeyer, P. A., Balsamo, G., Blyth, E. M., Morrison, R. & Cooper, H. M. Land-atmosphere interactions exacerbated the drought and heatwave over northern Europe during summer 2018. *AGU Advances* **2**, e2020AV000283 (2021).
61. Forsyth, G. G., Le Maitre, D. C., Smith, J. & Lotter, D. *Upper Berg River Catchment (G10A) Management Unit Control Plan*. (Natural Resources Management (NRM) Department of Environmental Affairs, 2016).
62. Coetsee, C., Gray, E. F., Wakeling, J., Wigley, B. J. & Bond, W. J. Low gains in ecosystem carbon with woody plant encroachment in a South African savanna. *Journal of Tropical Ecology* **29**, 49-60, doi:10.1017/s0266467412000697 (2012).
63. Stevens, N., Erasmus, B. F., Archibald, S. & Bond, W. J. Woody encroachment over 70 years in South African savannahs: overgrazing, global change or extinction aftershock? *Philos Trans R Soc Lond B Biol Sci* **371**, doi:10.1098/rstb.2015.0437 (2016).
64. Venter, Z. S., Cramer, M. D. & Hawkins, H. J. Drivers of woody plant encroachment over Africa. *Nat Commun* **9**, 2272, doi:10.1038/s41467-018-04616-8 (2018).
65. Terrer, C. *et al.* A trade-off between plant and soil carbon storage under elevated CO2. *Nature* **591**, 599-603, doi:10.1038/s41586-021-03306-8 (2021).
66. Pascale, S., Kapnick, S. B., Delworth, T. L. & Cooke, W. F. Increasing risk of another Cape Town "Day Zero" drought in the 21st century. *Proc Natl Acad Sci U S A*, doi:10.1073/pnas.2009144117 (2020).
67. Thomas, A. *et al.* Global evidence of constraints and limits to human adaptation. *Regional Environmental Change* **21**, doi:10.1007/s10113-021-01808-9 (2021).
68. Dow, K., Berkhout, F. & Preston, B. L. Limits to adaptation to climate change: a risk approach. *Current Opinion in Environmental Sustainability* **5**, 384-391, doi:10.1016/j.cosust.2013.07.005 (2013).

# Figures

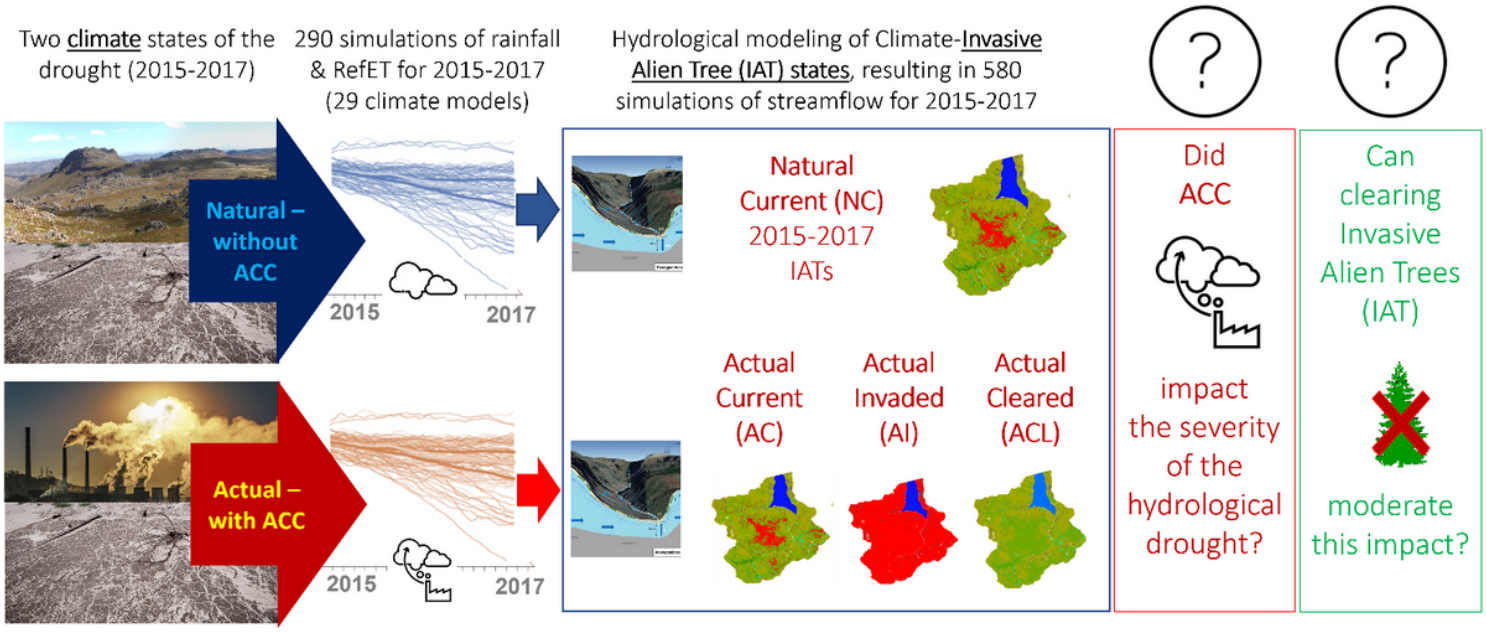


**Figure 1**

Modelling set-up for joint multi-model probabilistic event attribution (climate and IAT states) applied in this paper. Showing one subcatchment as an example: the Upper Berg Dam. The left two panels illustrate the simulations of climate variables for the Cape Town Day Zero Drought under today's climate (Actual) and a counterfactual climate (Natural) with human-induced drivers removed. The middle panel shows the three different Invasive Alien Tree (IAT) states resulting in hydrological modelling of four coupled climate-IAT states: Natural Current (NC), Actual Current (AC), Actual Invaded (AI), Actual Cleared (ACL). This then enabled us to attribute the relative contribution of anthropogenic climate change and catchment IAT state on hydrological drought severity; and the extent to which management of IATs can reduce the impact of anthropogenic climate change (last two panels).

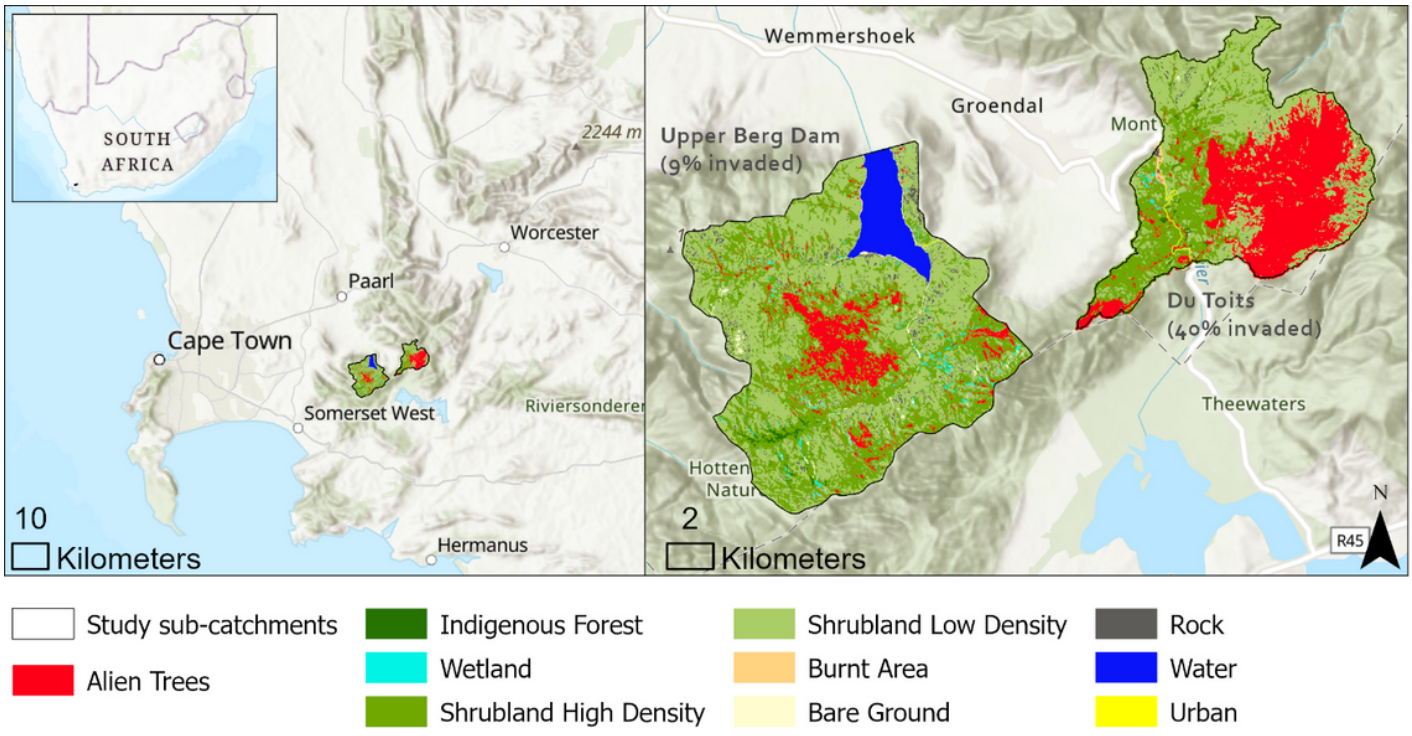

## Figure 2

Study subcatchments. Mountainous subcatchments, the Upper Berg and Du Toits, critical for water supply to the City of Cape Town in South Africa, and the level of Invasive Alien Tree infestations during the drought period (as described in30).

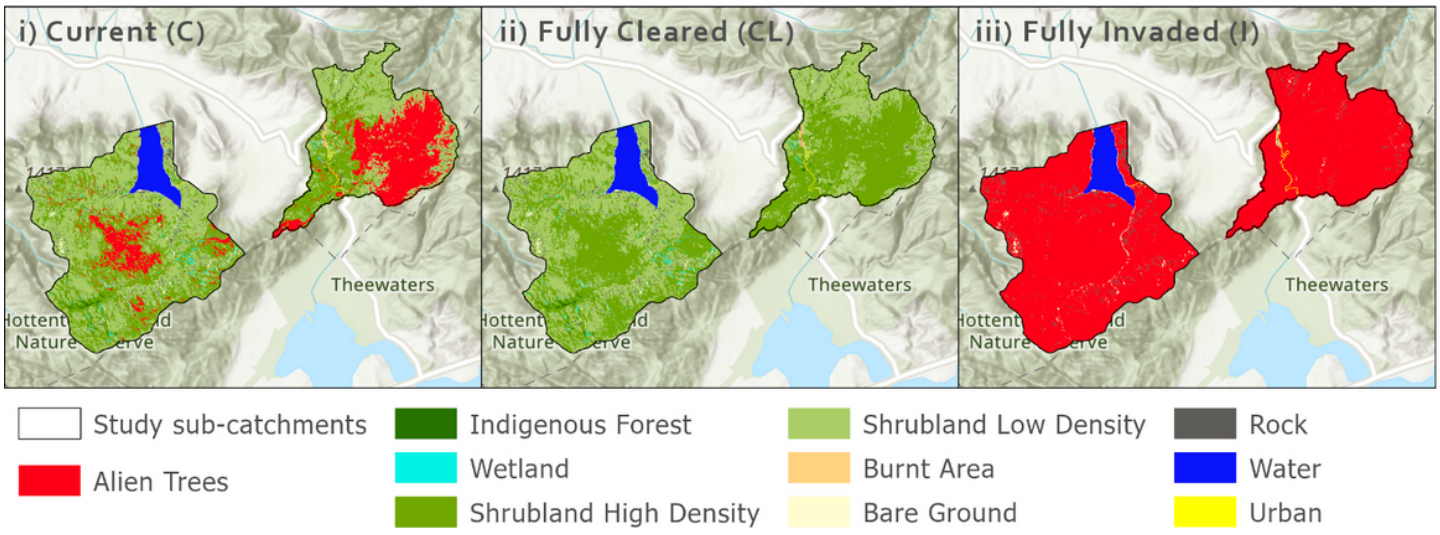


## Figure 3

Invasive Alien Tree (IAT) states. The three IAT landscape states used in the hydrological modelling i) Current (C) state which reflects invasion levels present during the drought (2015-2017); ii) Fully Cleared (CL) state representing all IATs cleared; and iii) fully Invaded (I) state representing lack of maintenance of cleared areas.

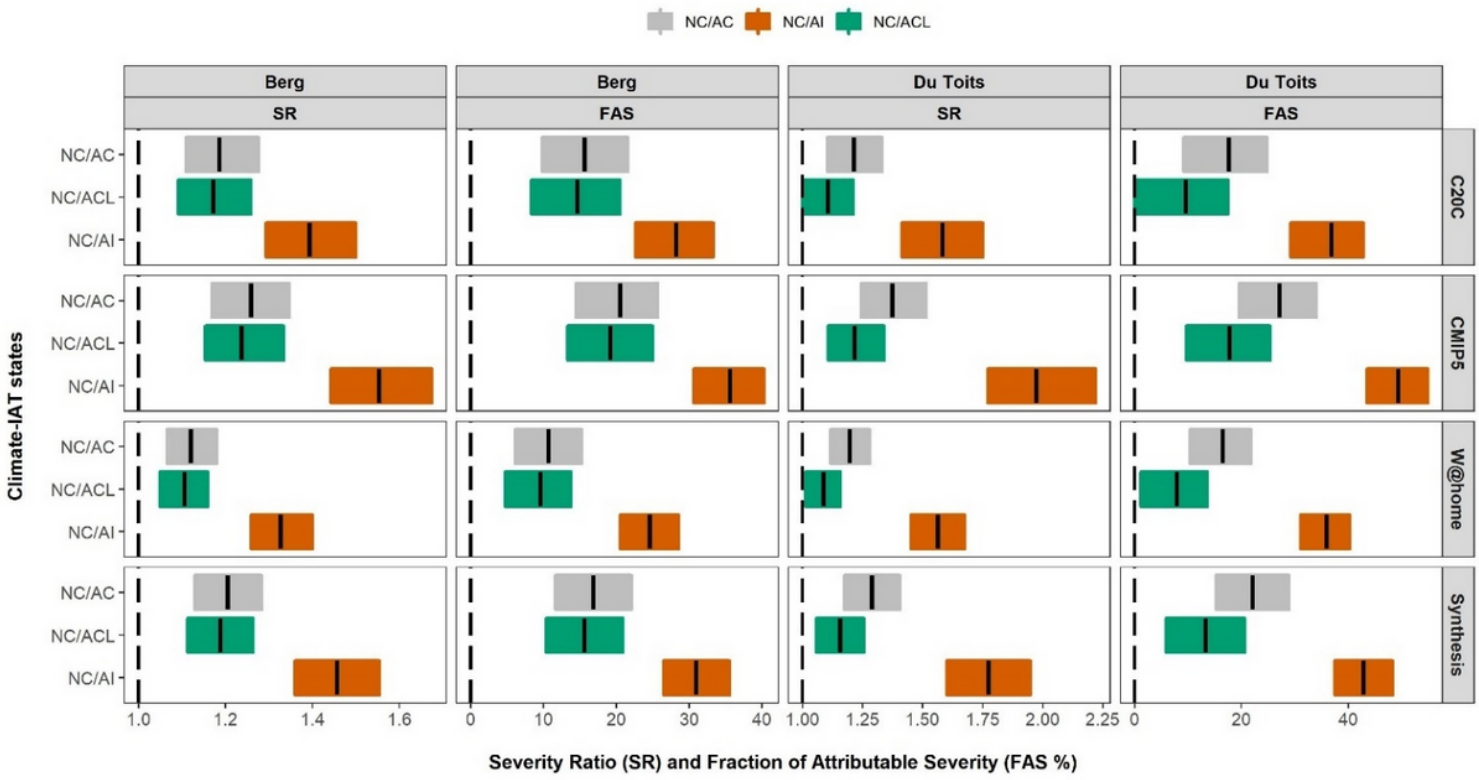


## Figure 4

Attributable hydrological drought severity to anthropogenic climate change. The severity (Severity Ratio (SR) and Fraction of Attributable Severity (FAS)) of the drought attributable to anthropogenic climate change (NC/AC) and the role of Invasive Alien Tree management or the lack thereof on modulating this impact. NC/ACL: clearing the actual invasion experienced during the drought years (9% - Upper Berg; 40% - Du Toits), NC/AI: allowing the subcatchment to become fully (100%) invaded. Climate model experiments (three top horizontal panels) show the median of the bootstrapped ensemble means with 95% quantiles (0.025 - 0.975 quantiles, referred to as 95%CI) and the synthesis (bottom panel) shows the mean of the model experiment medians, with equal weighting and 95% confidence intervals generated using the pooled standard deviation of the climate model experiments. NC = Natural Current; ACL = Actual Cleared; AI = Actual Invaded.

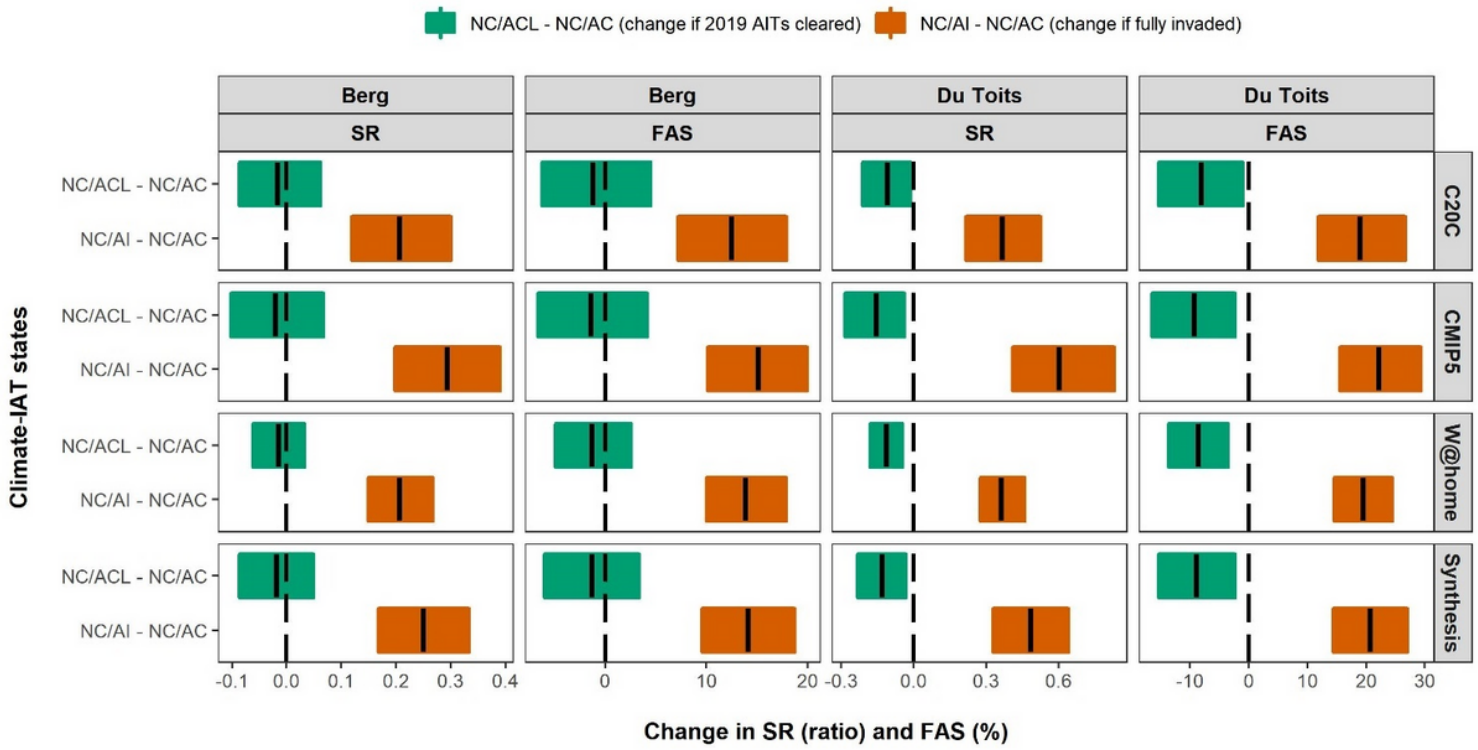


**Figure 5**

Change in attributable hydrological drought severity to anthropogenic climate change due to Nature-based Solutions. Median change in the Severity Ratio (SR) and Fraction of Attributable Severity (FAS) (with 95% confidence intervals) for the Upper Berg and Du Toits due to Invasive Alien Tree management (NC/ACL - NC/AC) or the lack thereof (NC/AI-NC/AC) (see Table 3 in section 2.1). Climate model experiments (three top horizontal panels) show the median of the difference between bootstrapped ensemble means with 95% quantiles (0.025 - 0.975 quantiles, referred to as 95%CI) and the synthesis shows the mean of the model experiment medians, with equal weighting and 95% confidence intervals generated using the pooled standard deviation of the climate model experiments. NC = Natural Current; ACL = Actual Cleared; AI = Actual Invaded.

# Supplementary Files

This is a list of supplementary files associated with this preprint. Click to download.

- SupplementaryMaterial13092021.docx